Applied Energy 149 (2015) 133–147

Contents lists available at ScienceDirect

Applied Energy

journal homepage: www.elsevier.com/locate/apenergy

Systems optimization model for energy management of a parallel HPGR crushing process

B.P. Numbi *, X. Xia

Centre of New Energy Systems, Department of Electrical, Electronic and Computer Engineering, University of Pretoria, Pretoria 0002, South Africa

HIGHLIGHTS

- Systems optimization control of a parallel HPGR crushing process is modeled.
- A daily energy cost saving of about 41.93% is achieved through optimal rolls speed control.
- Energy saving of 1.87% is achieved under different efficiency conditions of the parallel HPGRs.
- Energy saving of 4.5% is achieved for every decrement of 0.2 N/mm^2 in rolls pressure.
- A small decrement of 0.2 N/mm^2 in rolls pressure has a minor effect on the product quality.

ARTICLE INFO

Article history:
Received 27 October 2014
Received in revised form 13 March 2015
Accepted 25 March 2015

Keywords:
Systems optimization model
Energy management
Parallel HPGR crushing process
Time-of-use tariff

ABSTRACT

This work proposes a systems optimization control model for energy management of a parallel crushing process made up with high-pressure grinding rolls (HPGR) machines. The aim is to reduce both energy consumption and cost through optimal control of the process and load shifting, respectively. A case study of a copper crushing process is solved under three scenarios in order to evaluate the effectiveness of the developed model. Simulation results show that 41.93% energy cost saving is achieved through load shifting by coordinating the rotational speed of HPGRs. It is further shown that the energy saving can be achieved when the two HPGRs are not operated with equal overall efficiency, but also through a small decrement in rolls operating pressure. In the first case, 1.87% energy saving is obtained while in the last case, about 4.5% energy saving is achieved for every decrement of 0.2 N/mm^2 in rolls operating pressure without significant change in product quality.

1. Introduction

Systems optimization is widely employed in several industrial processes as a supervisory control system at the upper control layer. It aims at optimally adjusting in real-time, the set points of the regulatory control system at the lower control layer by minimizing or maximizing a given performance index of the process.

Depending on the control objective to be achieved on a process, several performance indices can be optimized. These are, for instance, the maximization of the energy efficiency, minimization of the energy cost, maximization of the total plant throughput, minimization of the downtime, maximization of the product quality, minimization of emissions, etc. Various algorithms can be embedded within the supervisory control system in order to achieve systems optimization of processes.

In general, systems optimization can be classified in two main categories depending on the level of automation. The first one is referred to as the open loop systems optimization where for a given control horizon, the optimization model is solved once (usually offline) and the optimal set points obtained are manually entered into the regulatory control system. The other one is the closed-loop systems optimization where the optimization model is solved online and the optimal set points are automatically entered into the regulatory control system.

Traditionally, in mining industries, systems optimization has been successfully applied to grinding circuits while maximizing either the milling circuit throughput or the grinding process profit. In Ref. [1], for instance, the milling circuit throughput is maximized using the "IF-THEN" rule-based algorithm. The obtained results show an improvement of the milling throughput by approximately 5%. In Ref. [2], a linear programming supervisory control is employed to maximize the grinding circuit throughput, while in Ref. [3], the grinding circuit throughput is maximized using an

* Corresponding author. Tel.: +27 12 420 5789; fax: +27 12 362 5000.
E-mail address: papy.numbi@up.ac.za (B.P. Numbi).

http://dx.doi.org/10.1016/j.apenergy.2015.03.129
0306-2619/

Nomenclature

N	rolls rotational speed (rpm)
V	rolls peripheral speed (m/s))
R_P	rolls operating pressure (N/mm^2)
F	compression force (kN)
P_{net}	HPGR net mechanical power (kW)
P_{mech}	HPGR total mechanical power (kW)
P_{el}	HPGR total electrical power (kW)
J_E	HPGR electrical energy consumption (kW h)
J_C	HPGR electrical energy cost (currency)
c	proportional constant of no-load power (kW/rpm)
T_{FB}	fresh feed rate to the HPGR feed bin (t/h)
T_f	fresh feed rate to the HPGR (t/h)
T_p	product rate or throughput rate (t/h)
$T_{SC\text{-}OV}$	oversize flow rate (t/h)
$T_{SC\text{-}UD}$	undersize flow rate (t/h)
α_{IP}	inter-particle compression angle (°)
S_0	rolls gap (m)
D	rolls diameter (m)
L	rolls length or width (m)
δ	ore band density at the extrusion zone (t/m^3)
ρ_a	feed bulk density (t/m^3)
A, A_1, b, b_1, a_x, b_x	constants of model fittings
t_0 and t_f	initial and final time of the control horizon (h)
$p(t)$	time-based electricity price (currency/kW h)
η	overall drive efficiency
n	total number of HPGRs in parallel
t_s and j	sampling period (h) and jth sampling interval
N_s	total number of sampling intervals
$p(t)$	time-based electricity price (currency/kW h)
η	overall drive efficiency
n	total number of HPGRs in parallel
t_s and j	sampling period (h) and jth sampling interval
N_s	total number of sampling intervals
p^j	electricity price at jth sampling interval (currency/kW h)
F_x	x% passing size of the feed material (m)
P_x	x% passing size of the product material (m)
P_{max}	maximum size of product particle (m)
S_x	x% product size reduction ratio index (–)
M_{FB}	mass of ore in the crusher bin (t)
M^0_{FB}	initial value of M_{FB} (t)
M^{target}_{PS}	target of total ore mass production (t)
min and max	minimum and maximum of the variable

expert system based on fuzzy logic where an increase of 10% in feed tonnage is achieved. On the other hand, in Refs. [4,5], the cost function to be maximized is taken as the grinding circuit profit instead of the grinding circuit throughput as in Refs. [1–3]. The Hooke and Jeeves search routine algorithm is used in Ref. [4], while in Ref. [5], the model predictive control (MPC) is implemented.

However, due to the continual increase of energy cost, the importance of using systems optimization in minimizing the energy cost of material handling equipment in mining industries is shown in research works such as [6–9], while in Ref. [10], systems optimization is used for minimal energy cost of a primary jaw crushing process in deep mines.

In chemical industries, systems optimization is studied in Ref. [11] for throughput maximization in a gas processing plant and in Ref. [12] for fuel cost minimization of a sugar and ethanol heat and power system. An MPC strategy is adopted in Ref. [11] while in Ref. [12], a model adaptation and gradient correction strategy is applied.

Systems optimization is also used for energy cost minimization of water pumping processes in Refs. [13–16].

Refs. [7,8,10,15] are those where open loop systems optimization is applied, while in Refs. [1–6,9,11–14,16], a closed-loop systems optimization is applied.

Mineral processing is one of the biggest electricity consumers worldwide. It is reported in Ref. [17] that about 5% of the total electrical energy produced in the world, is consumed by mineral processing circuits, of which 80% goes to comminution process (crushing and grinding). Comminution is the first operation in mineral processing whereby the coarse ore coming from mines, usually referred to as run-of-mine (ROM) ore, is fragmented into particles with reduced or smaller size in order to extract the valuable minerals. Different type of crushers are used for mineral processing depending on the ore characteristics and plant throughput capacity to be achieved. In primary crushing station for instance, jaw and gyratory crushers are generally employed to reduce large amount of coarse and hard ROM ore from larger size, say 0–1000 mm down to 0–250 mm. The primary crushing operation is done either in underground mines or surface mines. This is followed by a secondary crushing station usually at surface mines, where crushing machines such as cones crushers are used to further reduce the hard ore from 0–250 mm down to less than 70 mm. From this stage, the fragmented ore is further reduced in tertiary crushing station, from 0–70 mm down to 0–12 mm. The tertiary crushing station is usually based on cone crushers or vertical shaft impact crushers. The fragmented ore product from the crushing plant is thereafter reduced in very smaller particles say, from 0–12 mm down to the range of 50–100 μm, in milling/grinding circuits by grinding machines to allow mineral recovery process [18].

While comminution takes about 80% of the overall energy consumption of the processing plant, this is known to be an inefficient process. In grinding circuits for instance, the efficiency of tumbling mills such as balls mills, Autogenous Gringing (AG) mills, Semi-Autogenous Grinding (SAG) mills is as low as 1%, or less [19]. The High-Pressure Grinding Rolls (HPGR) machine is a type of roll crushers which has been newly designed and introduced in mineral comminution circuits as replacement of tertiary crushers, SAG mills, ball mills and rod mills, in order to increase the efficiency of mineral processing plants in terms of both energy consumption and throughput capacity [20–23]. Replacing the abovementioned machines with an HPGR machine in comminution circuits is part of equipment efficiency improvement category [24]. While efforts have been made to improve the comminution efficiency at equipment level in order to decrease the energy cost associated with the comminution process, more energy cost saving can be achieved at the operational level, especially when TOU electricity tariff is applied as the case in many mining industries. The energy management for cost minimization based on TOU electricity tariff has been successfully demonstrated in mining transportation systems [6–9] as previously discussed. However, the literature shows that there is little research works done in order to improve the energy management of comminution processes, and especially HPGR crushing processes with parallel machines.

In our previous work [10], although the energy management for cost minimization is studied in a crushing process, this has been limited to jaw crusher. While jaw crusher is a compressive crushing machine in which the rock/ore is fragmented based on

reciprocating motion [25], in HPGR crusher, the rock is fragmented by compression action between two counter-rotating rolls [20]. The main control variable in a jaw crusher is the closed-side setting while in HGPR, the rolls operating pressure and rolls speed are the main the control variables. HPGR crusher is not only a different crushing machine from jaw crusher due to its configuration and working principle, but also due to its location in the comminution circuit in the sense that jaw crusher is intended for first crushing circuit while HPGR is intended for last crushing circuit. It is turns out that the optimization model of HPGR crushing process is completely different from that of jaw crushing process.

In view of the aforementioned, this paper proposes a systems optimization model for energy management of a parallel HPGR crushing process. An open loop strategy is used with the performance index being the energy cost. The energy cost is taken as performance index in order to balance between energy cost reduction through TOU electricity tariff and energy reduction through optimal process control. A parallel structure of material processing machines or material handling equipment in mining industries is usually used for the purpose of higher systems reliability, facilitating the operation planning [26] but also to improve the systems maintenance and increase the throughput capacity of the plant. In this paper, HPGR machines in parallel structure are assumed to have different efficiency. In practice, this assumption is reasonable for several reasons. Firstly, if the machines are not equally rated, the efficiency of the bigger crushing machine might be higher than that of the smaller one due, for instance to the higher efficiency that big electric motor drives present compared to small electric motor drives [27].[1] Secondly, although equally rated, the working conditions of the machines in parallel might be technically different from each other and hence, leads to their efficiency discrepancy during operation. This is the case with the HPGR machine where the ore feeding characteristics, especially, the feed size distribution affect its efficiency. In this case, therefore, the role of systems optimization would be to lower the loading level of the HPGR machine with lower efficiency and operate the one with higher efficiency at higher loading level in order to improve the overall energy efficiency of the process. the control/decision variables of the systems optimization developed in this work are the rolls operating pressure, HPGR rotational speed and the HPGR feed rate.

This paper is organized as follows: Section 2 presents the performance model of HPGR; Section 3 gives the systems optimization control model of the parallel HPGR crushing process. A case study is discussed in Section 4 in order to evaluate the effectiveness of the developed model through the obtained simulation results. Finally, the conclusion of the work done is given in Section 5.

2. Performance model of the HPGR

Before applying systems optimization to any energy system, its performance model needs to be expressed in terms of the control/decision variables. Hence, in this section, different performance indices of the HPGR are derived and expressed in terms of the control variables.

2.1. Overview of the HPGR machine

The operation principle of the HPGR is explained in Ref. [20]. As can be seen in Fig. 1, the ore material is force-fed into the machine from the top and crushed by compression breakage action between two counter-rotating rolls. Although the two rolls rotate at the same speed N, one of them, referred to as a fixed roll, rotates on a fixed axis while the other, referred to as a moveable or floating roll, is allowed to move linearly with a pressing force applied to it. Hence, in order to achieve material size reduction, the floating roll is forced up against the ore material found in the gap formed by the two rolls using a hydraulic oil cylinder system [20].

The two main variables or flexible operating parameters that influence the HPGR performance, namely, the energy consumed, throughput rate and product quality, are the rolls rotational speed N and the rolls operating pressure R_P [28]. In practice, the HPGR speed N is automatically adjusted through a variable speed drive (VSD) system while the rolls operating pressure R_P is automatically adjusted through a hydraulic oil cylinder system as previously mentioned. The feed rate T_f is considered as a third control variable in order to continuously equal the HPGR throughput rate T_p. For tertiary crushing process, the feeding control is usually done through belt conveyors equipped with a VSD system as opposed to primary crushing processes where the feeding control is usually based on vibrating grizzly feeders or apron feeders equipped with a VSD system due to the coarse characteristics of the feed ore/rock material.

2.2. Formulation of performance indices

As discussed earlier, systems optimization of any crushing process is traditionally based on one of the three performance indices: energy consumption, throughput rate and product quality. However, due to the continual increase of electricity price, the energy cost is becoming a major concern in mining industries. A new performance index is therefore progressively introduced in mineral processing circuits. This consists of the cost associated with the energy consumption of the processing machines, while traditional performance indices are considered as constraints. Although, the performance prediction model of the HPGR has been analytically derived in Ref. [28], this is not explicitly expressed in terms of the control variables. Hence, one of the objectives in this work is to express all the performance indices of the HPGR as a function of the control variables, suitable for systems optimization.

2.2.1. Energy model

In order to obtain the energy consumption and energy cost expressions of HPGR, its electrical power consumption has first to be formulated. In Ref. [28], the net mechanical power draw model of the HPGR is expressed as a function of the compression force, F (kN), the inter-particle compression angle, α_{IP} and rolls peripheral speed, V (m/s) as follows:

$$P_{net} = 2F \sin\left(\frac{\alpha_{IP}}{2}\right) V. \tag{1}$$

Due to the fact that the angle $\frac{\alpha_{IP}}{2}$ is small [28], Eq. (1) can be simplified to Eq. (2) by using Taylor series expansion around zero (also called MacLaurin series expansions) of the term $\sin\left(\frac{\alpha_{IP}}{2}\right)$.

$$P_{net} = FV\alpha_{IP}. \tag{2}$$

The inter-particle angle α_{IP} in Eq. (2) has been found to vary with the rolls gap, s_0 as [28,25]:

$$\cos\alpha_{IP} = \frac{1}{2D}\left[(s_0 + D) + \sqrt{(s_0 + D)^2 - \frac{4Ds_0\delta}{\rho_a}}\right], \tag{3}$$

or

$$\cos\alpha_{IP} = \left[1 - \left(\frac{\delta}{\rho_a} - 1\right)\frac{s_0}{D}\right], \tag{4}$$

where the rolls gap s_0 is linked to the rolls operating pressure R_P through an exponential function of the form [29]:

[1] ABB, Technical note-IEC 60034-30-1 Standard on efficiency classes for low voltage AC motors, <http://www.abb.com> [Last accessed: 09 March 2015].

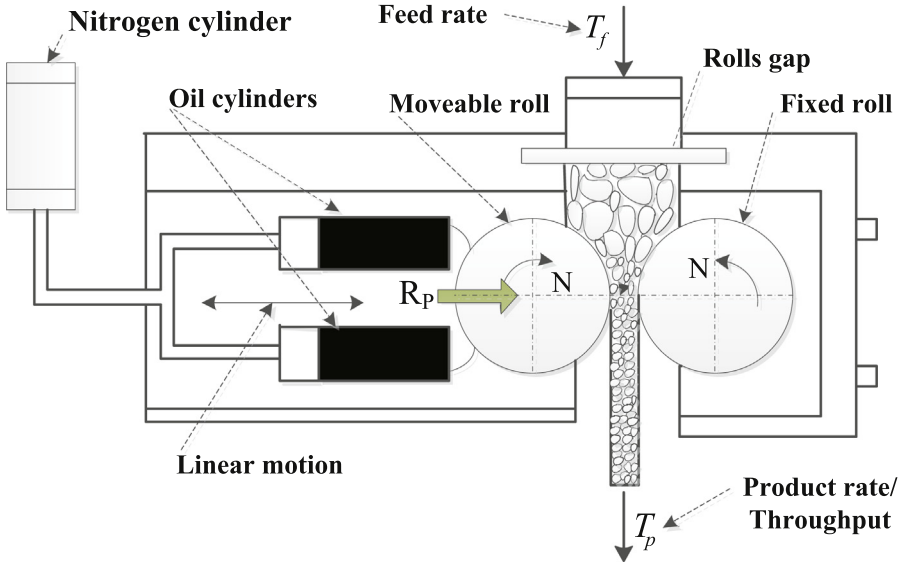

Fig. 1. Cross-sectional representation of HPGR (adapted from [20]).

$$s_0 = AR_P^{-b}. \tag{5}$$

The compressive force F (kN) is expressed in terms of the rolls operating pressure R_P (N/mm^2) as follows (adapted from [28]):

$$F = 1000R_P\frac{D}{2}L. \tag{6}$$

Hence, after converting the rolls peripheral speed, V (m/s) to rotational speed, N (rpm), using the relationship, $V = \frac{ND\pi}{60}$ and substituting Eqs. (3)–(6) in Eq. (2), the HPGR net mechanical power consumption can be finally expressed as function of the two flexible operating parameters (control variables), N and R_P as follows:

$$P_{\text{net}} = kNR_Pf(R_P), \tag{7}$$

where $k = \frac{25\pi}{3}D^2L$ and

$$f(R_P) = \begin{cases} \cos^{-1}\left(\frac{1}{2D}\left[\left(AR_P^{-b}+D\right) + \sqrt{\left(AR_P^{-b}+D\right)^2 - \frac{4DAR_P^{-b}\delta}{\rho_a}}\right]\right), \\ \text{or} \\ \cos^{-1}\left[1-\left(\frac{\delta}{\rho_a}-1\right)\frac{AR_P^{-b}}{D}\right]. \end{cases}$$

To obtain the total mechanical power consumption of the HPGR machine, the no-load power consumption needs to be added to the net mechanical power model given by Eq. (7). The no-load power, which is the power consumed by the HPGR when no material is being fed in, can be expressed as a function of the speed. Since both crushing and grinding machines behave generally as constant loads, their torque characteristics (torque versus speed) is almost constant for a given loading level.[2] Knowing that the mechanical power is proportional to the rotational speed, the mechanical power of the HPGR can be therefore approximated to a linear function of the speed with the proportional constant being the torque demand. This is proven by Eq. (7) where it is seen that for a given rolls operating pressure, the HPGR mechanical power is proportional to its speed. It is therefore found reasonable to assume in this work, that the HPGR no-load power follows the trend of the full load power (shaft power). The expression of the total mechanical power consumption of the HPGR is therefore written as follows:

$$P_{\text{mech}} = kNR_Pf(R_P) + cN, \tag{8}$$

where c is the proportional constant of no-load power, which is in reality the HPGR no-load torque. The least squares (LSQ) parameter estimation algorithm [30] can be used to estimate the coefficient c based on either field test data or manufacturer's data. At least one experimental data is needed to estimate the value of c when the HPGR crusher is operated under no-load conditions. This means that c can easily be determined if the no-load power consumption of the HPGR crusher is known at the nominal rotational speed N.

Finally, the electrical power consumption of the HPGR is expressed as:

$$P_{\text{el}}(N, R_P) = \frac{1}{\eta}(kNR_Pf(R_P) + cN), \tag{9}$$

where η is the overall drive efficiency, composed of electric motor drive efficiency, drive coupling efficiency and gearbox (speed reducer) efficiency. The total electrical energy, J_E, consumed during the time period between t_0 to t_f is expressed as below:

$$J_E = \int_{t_0}^{t_f}\sum_{i=1}^{n}P_{\text{el}}(N(t), R_P(t))dt. \tag{10}$$

With a given electricity price, $p(t)$, the total electrical energy cost, J_C, during the same time period between t_0 to t_f can be estimated as follows:

$$J_C = \int_{t_0}^{t_f}\sum_{i=1}^{n}P_{\text{el}}(N(t), R_P(t))p(t)dt. \tag{11}$$

2.2.2. Throughput model

The HPGR throughput $T_p(t/h)$ is expressed in [28] as function of the linear speed V and rolls gap s_0 as:

$$T_p = 3600\delta s_0LV. \tag{12}$$

By converting the linear speed V to rotating speed N and substituting Eq. (5) in Eq. (12), the HPGR throughput can be expressed in terms the two variable controls as given below:

$$T_p = k_1NR_P^{-b}, \tag{13}$$

where $k_1 = 60\pi ALD\delta$.

[2] Bill Horvath (2013), Selecting motor controls for mining process torque demands, <http://www.wmea.net> [Last accessed: 03 July 2014].

The HPGR power consumption can also be expressed as a function of the throughput and rolls operating pressure by substituting Eq. (12) or Eq. (13) into Eq. (1) to eliminate the rolls speed.

2.2.3. Product quality model

The performance index of the product quality model of any crushing or grinding process is generally a parameter that affects the product particle size distribution from the comminution machine. These are for instance, the 50% (or average) product size reduction ratio index, $S_{50\%}$, the 80% product size reduction ratio index, $S_{80\%}$, the 50% (or average) passing size of the product, $P_{50\%}$, the 80% passing size of the product, $P_{80\%}$ [31] and the maximum product particle size, $P_{\max}$ [29]. All these parameters are based on empirical models. For HPGR, these product quality indices have been found to be more dependent on the rolls operating pressure than the rolls speed [32]. When the rolls operating pressure is within its operating range, for a given moisture amount in the feed product, the product size reduction ratio index can be expressed as function of the rolls operation pressure through a linear relationship as [31]:

$$S_x = \frac{F_x}{P_x} = a_x R_P + b_x, \tag{14}$$

where x is the $x\%$ passing percentage (50%) or (80%). It can be seen that for a given passing size of the feed material, F_x, the P_x can also be derived from Eq. (14) as:

$$P_x = \frac{F_x}{a_x R_P + b_x}. \tag{15}$$

The maximum product particle size is expressed by an hyperbolic relationship as follows [29]:

$$P_{\max} = A_1 R_P^{-b_1}. \tag{16}$$

2.3. Energy model analysis

Fig. 2 depicts the 3D analytical performance of HPGR in terms of the power consumption (left-hand side graph) and the throughput rate (right-hand side graph). The data of this HPGR is found in Ref. [28]. The analysis of this figure shows that both rolls speed and rolls operating pressure have considerable effect on the HPGR power consumption, while the throughput rate is more dependent on the rolls speed than the rolls operating pressure. It therefore is seen that the HPGR power consumption can be minimized by either reducing the rolls speed or the rolls operating pressure. However, the reduction of the rolls speed will unfortunately result in HPGR throughput rate decrease. On the other hand, if the rolls operating pressure is decreased for power consumption minimization, the product quality performance will decay as this will lead to smaller reduction ratio (see Eq. (14)) or bigger product size (see Eq. (15)).

The analysis above clearly shows that the optimization of an HPGR process circuit is in reality a multi-objective problem due to the trade-off between the three traditional performance indices.

In comminution processes, when the product quality index is set as a requirement or constraint, the two remaining performance indices (power consumption and throughput rate) are combined in a unique performance index whereby the two performance indices can be simultaneously optimized. This is referred to as the specific energy consumption, defined as the ratio between the power consumption and the throughput rate. Hence, minimizing the HPGR specific energy consumption means minimizing its power or energy consumption by maximizing its throughput rate. The specific energy consumption of HPGR is shown in Fig. 3. From this figure, it is seen that the variation in rolls speed has no effect on the HPGR specific energy consumption, while the increase in rolls operating pressure leads to an increase in specific energy consumption. This observation is also demonstrated through experimental results in Ref. [32]

From this, it can be observed that the only control variable affecting the specific energy consumption of the HPGR process is the rolls operating pressure. However, in practice, the rolls speed still to be taken as additional flexible operating parameter in order to control the HPGR throughput rate in such a way to continuously compensate for the feed rate change due to the upstream circuit schedule or load shifting scheme. It is noted that Figs. 2 and 3 represent the operating region of the above analyzed HPGR crusher where this machine can be operated under different operating points depending on the desired product quality (fixed by the rolls operating pressure) and throughput (fixed by the rolls speed) to be achieved at various periods.

3. Systems optimization model

3.1. Description of a parallel HPGR crushing circuit

As previously discussed, the HPGR machine is usually employed in comminution circuit, for replacement of primary grinding machines such as ball mills, AG mills and SAG mills or in the last stage crushing process such as tertiary and quaternary crushing. In this work, we consider a case where the HPGR machine is used in a last stage crushing station with a parallel configuration as

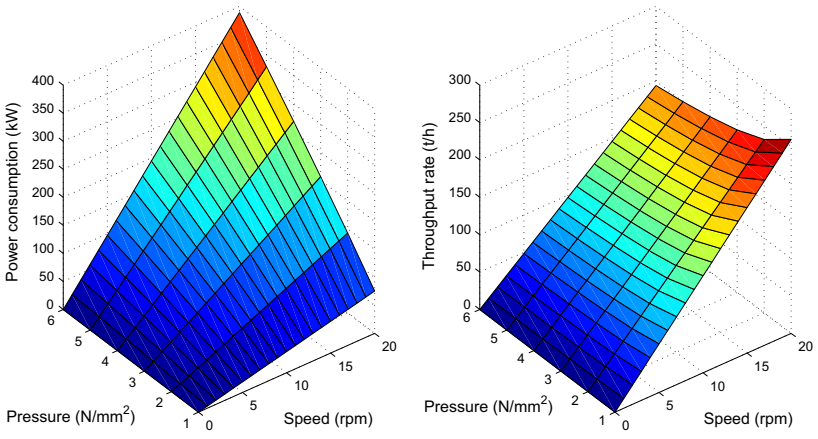

Fig. 2. 3D plots of the analytical models of power consumption and throughput rate of HPGR machine.

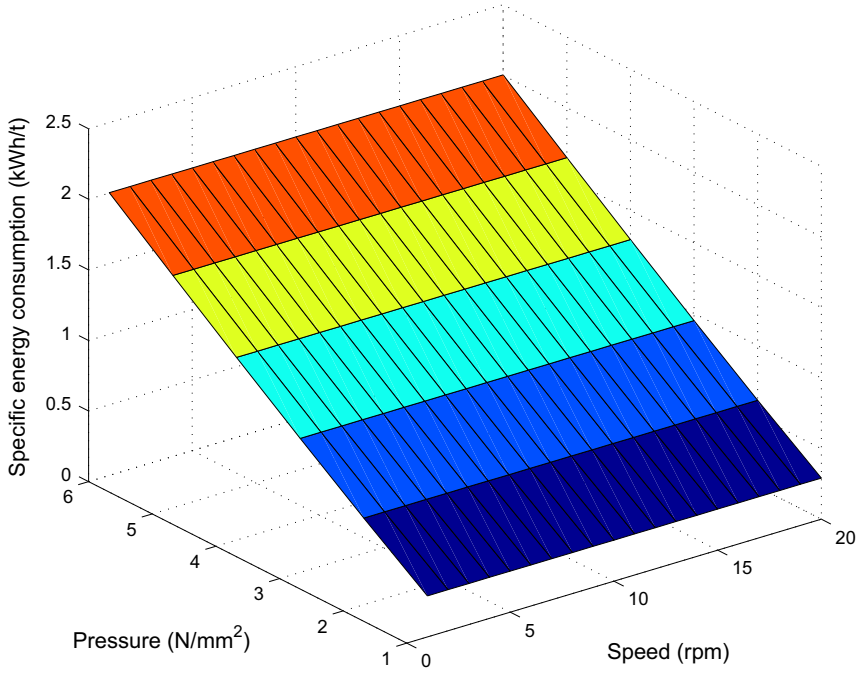

Fig. 3. 3D plot of the analytical specific energy model of HPGR machine.

shown in Fig. 4. The Vasilkovskoye gold mine in Central Asia is one of industrial examples where a parallel configuration with two Humboldt Wedag HPGR crushers has been operating since 2009 [33].

In a tertiary crushing process such as shown in Fig. 4, the ore material from the crusher bin is processed by the two parallel HPGRs, at fresh feed flow rates of T_{f_1} and T_{f_2}, respectively, before being discharged to the screens at flow rates of T_{p_1} and T_{p_2}, respectively. The upstream crusher bin is supposed to receive the ore material from a secondary crushing station at a feed flow rate of T_{FB}. During operation, the crushing bin is subject to certain maximum and minimum capacity limits of receptively, $M_{\mathrm{FB}}^{\max}$ and

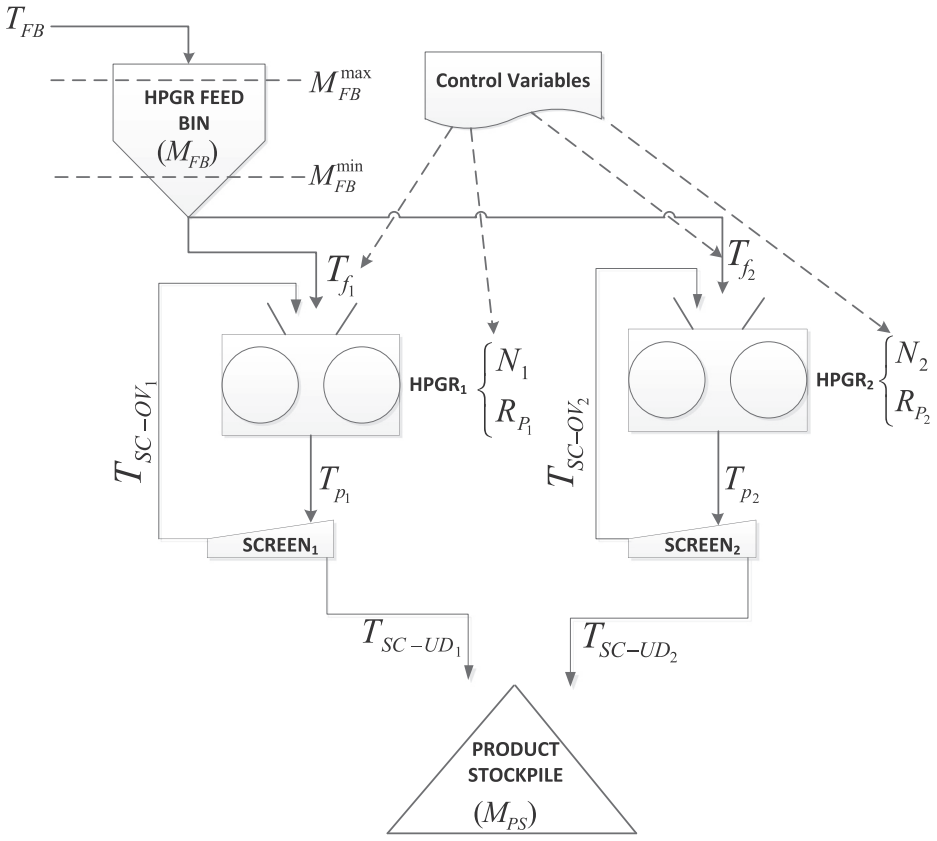

Fig. 4. Schematic of a two parallel HPGR crushing circuit.

M_{FB}^{min}. After the ore product is discharged to the screens for size control, the amount of ore material with size higher than the screen aperture, called screen oversize, is fed back or recirculated to the crusher bin, at flow rates of $T_{RC\text{-}OV_1}$ and $T_{RC\text{-}OV_2}$, respectively. The ore material with size less than the screen aperture, called screen undersize, goes to the downstream grinding stockpile, at flow rates of respectively, $T_{SC\text{-}UD_1}$ and $T_{SC\text{-}UD_2}$.

3.2. Objective function

The performance index considered in this work is the total energy cost to be minimized by taking advantage of the TOU electricity tariff. Hence, for n HPGRs in parallel, the objective function in Eq. (11) is discretized for simplicity purpose and expressed as:

$$\min \sum_{i=1}^{n}\sum_{j=1}^{N_s} P_{el_i}\left(N_i^j, R_i^j\right)p^j t_s, \tag{17}$$

where $t_s = \frac{t_f - t_0}{N_s}$.

3.3. Constraints

During operation, the parallel HPGR circuit is subject to physical and operational or technical constraints.

Physical constraints are physical limitations of crushing circuit equipment according to their design specifications. From Fig. 4, these are for instance, the bin upper level M_{FB}^{max}, to avoid ore material not overflowing, bin lower level M_{FB}^{min}, to avoid the bin running empty. Each HPGR also have limitations on rolls speed N, rolls operating pressure R_P, rolls gap S_0, and throughput rate T_p, which need to be maintained within a certain range based on design specifications.

On the other hand, operational or technical constraints are those which are directly linked to the HPGR crushing process for production maximization as well as product quality improvement. These are for instance, the mass balances in the HPGR and screens.

3.3.1. HPGR feed bin level limits

At any time, for n parallel HPGRs, the quantity of the ore stored or available in the HPGR feed bin can be calculated based on the first difference equation as follows:

$$M_{FB}^{j} = M_{FB}^{j-1} + t_s\left(T_{FB}^{j-1} - \sum_{i=1}^{n} T_{fi}^{j-1}\right). \tag{18}$$

Based on induction reasoning, the dynamics of the bin level can be expressed in terms of the initial level, M_{FB}^{0} as follows:

$$M_{FB}^{j} = M_{FB}^{0} + t_s\sum_{k=1}^{j}\left(T_{FB}^{k} - \sum_{i=1}^{n} T_{fi}^{k}\right). \tag{19}$$

The bin level constraints can therefore be written as:

$$M_{FB}^{min} \leqslant M_{FB}^{0} + t_s\sum_{k=1}^{j}\left(T_{FB}^{k} - \sum_{i=1}^{n} T_{fi}^{k}\right) \leqslant M_{FB}^{max}, \quad (1 \leqslant i \leqslant n;\ 1 \leqslant j \leqslant N_s). \tag{20}$$

3.3.2. HPGR variable limits

These are upper and lower bounds on each HPGR operational parameters. These constraints are given as follows:

$$\begin{cases} N_i^{min} \leqslant N_i^j \leqslant N_i^{max}, & (1 \leqslant i \leqslant n;\ 1 \leqslant j \leqslant N_s), \\ R_{P_i}^{min} \leqslant R_{P_i}^j \leqslant R_{P_i}^{max}, & (1 \leqslant i \leqslant n;\ 1 \leqslant j \leqslant N_s), \\ S_{0_i}^{min} \leqslant S_{0_i}^j \leqslant S_{0_i}^{max}, & (1 \leqslant i \leqslant n;\ 1 \leqslant j \leqslant N_s), \\ T_{P_i}^{min} \leqslant k_{1_i} N_i^j R_{P_i}^{-bj} \leqslant T_{P_i}^{max}, & (1 \leqslant i \leqslant n;\ 1 \leqslant j \leqslant N_s), \\ T_{f_i}^{min} \leqslant T_{f_i}^j \leqslant T_{f_i}^{max}, & (1 \leqslant i \leqslant n;\ 1 \leqslant j \leqslant N_s). \end{cases} \tag{21}$$

3.3.3. HPGR circuit operational requirement

These constraints are given as follows:

- Mass balance in HPGRs

For efficient operation of HPGR, the fresh feed rate should always equal the throughput rate in order to avoid the HPGR crushing zone from being obstructed. This constraint is given as:

$$T_{f_i}^j + T_{SC\text{-}OV_i}^j = T_{p_i}^j = k_{1_i} N_i^j R_{P_i}^{-bj}, \quad (1 \leqslant i \leqslant n;\ 1 \leqslant j \leqslant N_s). \tag{22}$$

By relating the throughput rate T_p to the screen oversize flow rate $T_{SC\text{-}OV}$ through a ratio, referred to as recirculating mass ratio α, as $T_{SC\text{-}OV} = \alpha T_p$, Eq. (22) can be rewritten and expressed in terms of the control variables as follows:

$$\begin{aligned} T_{f_i}^j &= \left(1 - \alpha_i^j\right)T_{p_i}^j \\ &= \left(1 - \alpha_i^j\right)k_{1_i} N_i^j R_{P_i}^{-bj}, \quad (1 \leqslant i \leqslant n;\ 1 \leqslant j \leqslant N_s). \end{aligned} \tag{23}$$

- Throughput capacity requirement

Each mining operator has a daily, weekly, monthly or annually production target to be achieved on the crushing circuit. To ensure this, the total amount of ore crushed should be greater than or equal to the throughput capacity target (requirement), M_{SP}^{target}, stored in the product stockpile for a given period. This can be expressed as:

$$\sum_{i=1}^{n}\sum_{j=1}^{N_s} T_{SC\text{-}UD_i}^j t_s \geqslant M_{PS}^{target}. \tag{24}$$

The screen undersize flow rate $T_{SC\text{-}UD}$ can be written as $T_{SC\text{-}UD} = (1-\alpha)T_p$ knowing that $T_p = T_{SC\text{-}OV} + T_{SC\text{-}UD}$. With this, Eq. (24) can be rewritten and expressed as follows:

$$\sum_{i=1}^{n}\sum_{j=1}^{N_s}\left(1 - \alpha_i^j\right)k_{1_i} N_i^j R_{P_i}^{-bj} t_s \geqslant M_{PS}^{target}. \tag{25}$$

- Product quality requirement

The more practical product quality index can be considered to be the maximum particle size in the product, P_{max}. During HPGR operation, this should be kept smaller than a specified value, P_{max}^{spec}. According to Ref. [29], this constraint can be written as follows:

$$A_1 R_{P_i}^{-jb_1} \leqslant P_{max}^{spec}, \quad (1 \leqslant i \leqslant n;\ 1 \leqslant j \leqslant N_s). \tag{26}$$

4. Case study and simulation results

In order to demonstrate the feasibility of the proposed technique, an anonymous two parallel HRC™800 HPGR crushing process as shown in Fig. 4 is used for simulations under three different scenarios. The rock processed is the copper ore. The effectiveness of the proposed model is analyzed by comparing its simulation results to those of the current control technique considered as baseline. The current control technique is formulated as in Ref. [10]. For simplicity, an open circuit HPGR application is considered in all simulations, hence the recirculated material is zero ($\alpha = 0$). As previously discussed, in practice, the rolls operating pressure R_P is varied in such a way to yield a constant product quality requirement index for any change in material feed size. R_P is pre-

set to a constant value for a given constant feed size distribution, and hence the rolls rotational speed N and fresh feed rate T_f remain as the only control variables. Since the rolls operating pressure is fixed, the systems optimization model becomes a linear programming problem and hence, *linprog* function of Matlab Optimization Toolbox is used. The optimal results from *linprog* function of Matlab Optimization Toolbox are also compared to those obtained with the *opti* function of Opti Toolbox in order to further evaluate the effectiveness of the proposed model.

4.1. Data presentation

4.1.1. Time-of-use electricity tariff

Eskom Megaflex electricity tariff for larger industrial consumers is considered for simulations. The systems optimization control is assumed to be implemented only within the high-demand season (from June to August) weekday. The corresponding TOU electricity tariff is given as[3]:

$$p(t) = \begin{cases} p_o = 0.3656\ \text{R/kW h} & \text{if } t \in [0,6] \cup [22,24], \\ p_s = 0.6733\ \text{R/kW h} & \text{if } t \in [6,7] \cup [10,18] \cup [20,22], \\ p_p = 2.2225\ \text{R/kW h} & \text{if } t \in [7,10] \cup [18,20], \end{cases} \tag{27}$$

where p_o, p_s and p_p are respectively, the off-peak, standard and peak TOU electricity prices; R is the South African currency Rand and t is the time of any weekday in hours (from 0 to 24).

4.1.2. HPGR crusher and ore characteristics

The technical data for the two identical HPGRs are given as follows[4]: the installed electric power is 220 kW (300 hp) each; the rolls diameter D and width L are 800 mm and 500 mm, respectively; the maximum of the rolls rotational speed N is 32 rpm; the synchronous speed is 1800 rpm (4 poles squirrel cage induction motors at 60 Hz); the maximum of the rolls operating pressure R_P is 4.5 N/mm^2; the maximum feed size is 32 mm; the maximum of the throughput rate T_p is about 120 t/h (however, in this work, 110 t/h is used as maximum throughput rate). Although the motor synchronous speed of the HRC™800-series HPGR crusher is 1800 rpm at 60 Hz, in this work, the synchronous frequency is taken as 50 Hz as the case in South Africa; hence a synchronous speed of 1500 rpm for a 4 poles squirrel induction motor. With this, the gearbox reduction ratio is therefore of about 46.4:1 (with the rotor speed of the squirrel cage induction motor being about 1485 rpm for a slip of 1%). The motor considered is assumed to be a premium efficiency motor-IE3 whose efficiency is 95.4% for each 110 kW motor rating.[5] With a gearbox efficiency of 85% for medium-ratio helical-worm speed reducers (20:1 to 60:1) [34], and drive coupling efficiency of 99% [35], the overall drive efficiency is calculated as $0.954 \times 0.85 \times 0.99 = 80.28\%$. The no-load power is assumed to be 6% of the full power as compared to 3.75% for bigger HPGR crushers in Ref. [36]. Hence, the proportional constant of no-load power c is calculated as $\frac{220\ \text{kW} \times 0.8028 \times 0.06}{32\ \text{rpm}} = 0.33\ \text{kW/rpm}$. The characteristics of the copper ore used are as follows: the specific gravity (density) ρ is 2.7 t/m^3; the bulk density ρ_a of 1.6 t/m^3 and the maximum feed size is 30 mm.

4.1.3. HPGR feed bin

The fresh feed rate to the HPGR feed bin, T_{FB} is given in Tables 1–3. The capacity of the feed bin is 1875 t. In all simulations, the upper limit and lower limit of the feed bin are set, respectively, to 80% and 24% of the bin capacity. The initial ore level M_{FB}^0 is set to 64% of the bin capacity.

Table 1
Fresh feed rate for 24 h.

Time (h)	1	2	3	4	5	6	7	8
Feed rate (t/h)	135.5	135.9	136.8	137.6	138.0	138.9	139.3	139.7

Table 2
Fresh feed rate for 24 h (continued).

Time (h)	9	10	11	12	13	14	15	16
Feed rate (t/h)	140.6	141.4	141.8	142.3	141.4	140.6	139.7	138.5

Table 3
Fresh feed rate for 24 h (continued).

Time (h)	17	18	19	20	21	22	23	24
Feed rate (t/h)	130.0	138.9	139.7	141.4	140.6	138.9	137.2	136.3

4.2. Simulation results

The sampling period t_s of 10 min within a control horizon $[t_0, t_f]$ of 24 h and total production target M_{PS}^{target} of 3500 t are considered for all simulations.

4.2.1Case I: Systems optimization control with equal overall drive efficiency

In this scenario, the two HPGRs are assumed to have equal overall drive efficiency of $\eta_1 = \eta_2 = 80.28\%$. The rolls operating pressure is pre-set to 4.5 N/mm^2. The feasibility of the current control technique is shown in Fig. 5 while that of systems optimization control techniques based on *linprog* of Matlab Optimization Toolbox and *opti* of Opti Toolbox are, respectively, shown in Figs. 6 and 7. The performance of the two optimization techniques are compared in Fig. 8 and Tables 4–6. The dotted lines in Figs. 5–7 denote the maximum and minimum of the corresponding variable. It is shown that both current control and systems optimization control techniques operate the parallel HPGR under the given constraints.

However, on one hand, Fig. 5 shows that the current control scheme run the two HPGR crushers under almost constant speed, leading therefore to an even distribution of both fresh feed rate T_f and product (throughput) rate T_p along the 24 h control horizon. Also, it can be seen that current control chooses to run the first HPGR at high speed of around 26.5 rpm, which corresponds to its maximum loading level of 110 t/h. The second HPGR is therefore used as a buck up crushing machine with a lower loading level of about 36 t/h in order to meet the daily production target assigned to 3500 t. Owing to the fact that the crushing load is evenly distributed along the control horizon due to the lack of TOU tariff consideration, the energy cost reduction through load shifting cannot be achieved under the current control technique. Consequently, a high energy cost is incurred.

On the other hand, Figs. 6 and 7 show that both systems optimization control techniques run the two parallel HPGRs with equal loading level by shifting the load from peak time to off-peak and standard time in order to reduce the energy cost. The reason of the systems optimization controllers to run the two HPGRs with equal load is justified by the fact the two machines are assumed

[3] Eskom, Tariffs & Charges Booklet 2013/2014, <http://www.eskom.co.za> [Last accessed: 08 October 2014].
[4] Metso, HRC™800, <http://www.metso.com> [Last accessed: 08 October 2014].
[5] ABB, Technical note-IEC 60034-30-1 Standard on efficiency classes for low voltage AC motors, <http://www.abb.com> [Last accessed: 09 March 2015].

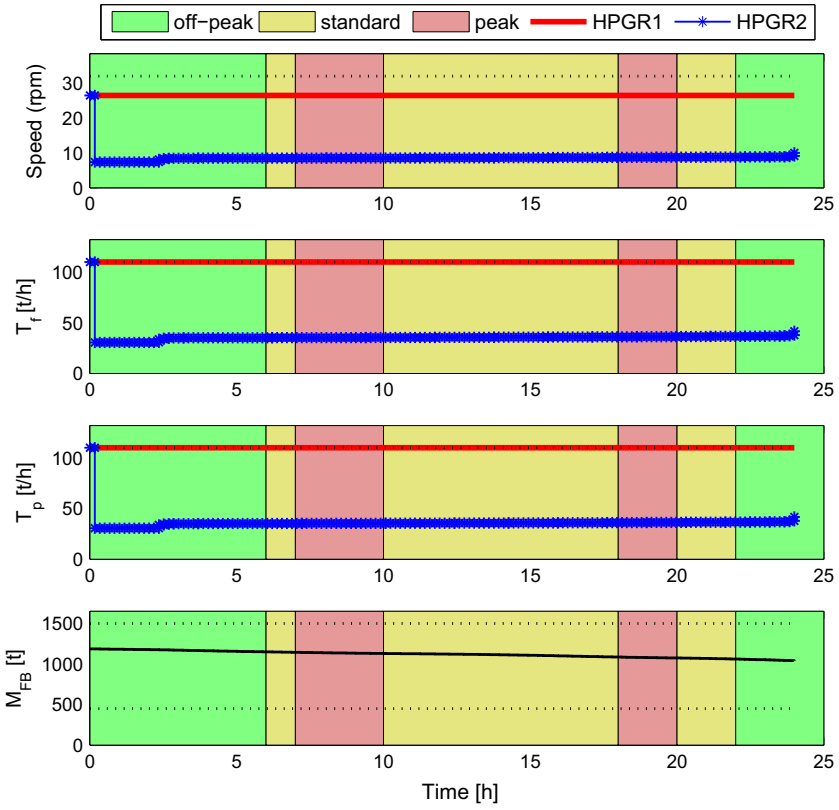

Fig. 5. Current control technique.

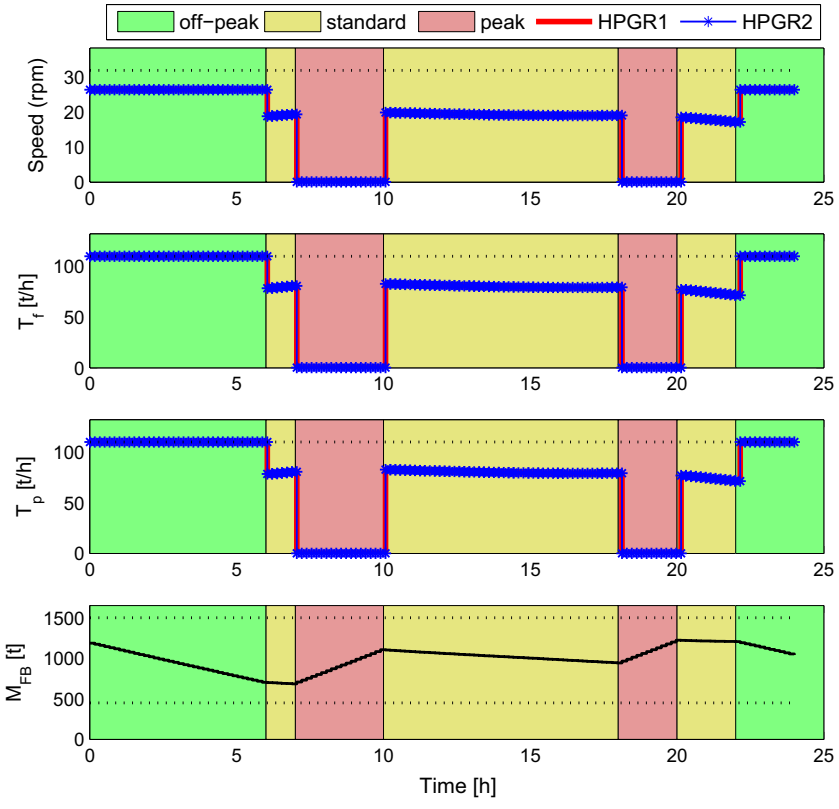

Fig. 6. Systems optimization control technique with equal overall drive efficiency, $\eta_1 = \eta_2 = 80.28\%$ using *linprog* function of Matlab Optimization Toolbox.

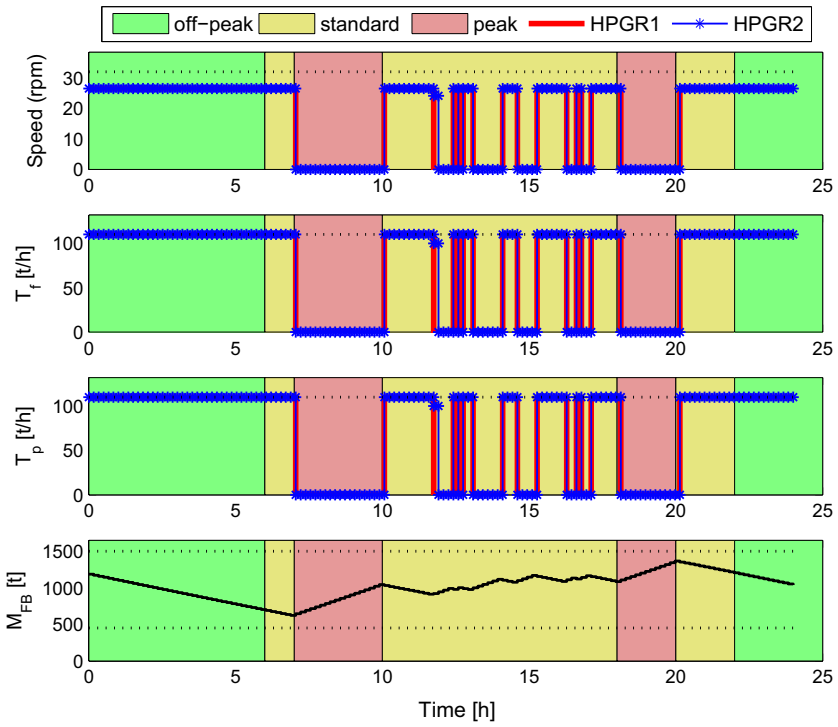

Fig. 7. Systems optimization control technique with equal overall drive efficiency, $\eta_1 = \eta_2 = 80.28\%$ using *opti* function of Opti Toolbox.

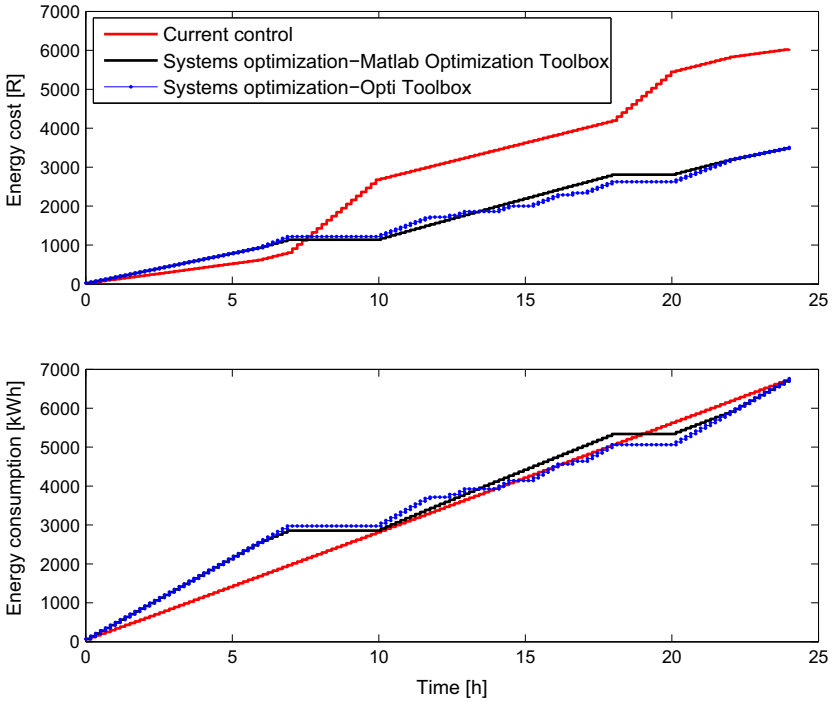

Fig. 8. Cumulative energy cost and consumption with equal overall drive efficiency, $\eta_1 = \eta_2 = 80.28\%$.

to have equal overall efficiency. In the current control, although the two HPGRs have equal overall efficiency, their loading levels are not necessary the same due to the fact that the energy model is not taken into account in the cost function.

The performance indices in terms of cumulative energy cost and energy consumption of both current control and systems optimization control techniques are presented in Fig. 8 and Tables 4–6. It is seen that at the end of the control horizon (24 h), the energy cost is sensibly reduced when systems optimization control techniques are used. About 41.93% energy cost saving is achieved with both systems optimization techniques. However, simulation results does not show any energy consumption

Table 4
Production and corresponding energy cost and consumption with equal overall drive efficiency, $\eta_1 = \eta_2 = 80.28\%$.

Technique	Production (t)	Energy cost (R)	Energy consumption (kW h)	Simulation time (s)
Current control	3500.2	6038.7	6761.8	/
Systems optimization using *linprog* function	3500.0	3506.3	6761.4	0.302
Systems optimization using *opti* function	3500.0	3506.3	6761.4	0.271

Table 5
Cost saving of systems optimization technique with equal overall drive efficiency, $\eta_1 = \eta_2 = 80.28\%$.

Technique	Specific energy cost (R/t)	Cost saving (%)
Current control	1.7252	/
Systems optimization using *linprog* function	1.0018	41.93
Systems optimization using *opti* function	1.0018	41.93

Table 6
Energy saving of systems optimization technique with equal overall, $\eta_1 = \eta_2 = 80.28\%$.

Technique	Specific energy consumption (kW h/t)	Energy saving (%)
Current control	1.9318	/
Systems optimization using *linprog* function	1.9318	0.00
Systems optimization using *opti* function	1.9318	0.00

reduction or energy saving. The reason is that the rolls operating pressure which is the main variable controlling the specific energy consumption of the HPGR, is constant in order to yield a constant required product size distribution.

Although both systems optimization techniques give the same performance as shown in Fig. 8 and Tables 4–6, the comparison of Fig. 6 and Fig. 7 reveals that the load profiles from the two techniques are different, especially during standard periods. It is shown that during standard periods, the systems optimization technique based on *linprog* function of Matlab Optimization Toolbox, smoothly operates each HPGR crusher at a reduced speed of about 19 rpm, corresponding to a loading level of about 80 t/h. With the *opti* function of Opti Toolbox, however, each HPGR crusher is frequently switched on and off from its maximum loading level of 110 t/h to its minimum loading level of 0 t/h, which in practice, may lead to extra energy consumption during the starting period of the machine. The high current required during starting periods will not only lead to extra energy consumption but also to the electrical stress on the electric motors, cables, transformers, breakers, transmission lines, etc. Moreover, the resulting high starting torque pulsations will generally lead to the mechanical stress on transmission shafts, bearings, mechanical drive coupling and vibrations of the concrete foundation supporting the HPGR crusher. However, as shown in Table 4, the optimal solutions when using *opti* function are obtained with less computational time.

4.2.2Case II: Systems optimization control with different overall drive efficiency

This scenario investigates the influence of the discrepancy between the overall efficiency of two parallel crushing machines, HPGR1 and HPGR2, during operation due to the unequal feeding characteristics of the two crushers, as discussed in Section 1. During the control horizon of 24 h, the first crusher, HPGR1, is assumed to run with a decreased overall efficiency of $\eta_1 = 76\%$ while the overall efficiency of the second crusher, HPGR2, is kept at its initial value of $\eta_2 = 80.28\%$. The rolls operating pressure of the two machines is also pres-set to 4.5 N/mm^2. Simulation results for this scenario are given in Figs. 9–11 and Tables 7–9. It can be seen from Fig. 9 that both systems optimization control techniques shifts the loads of the two HPGRs from peak time to off-peak and

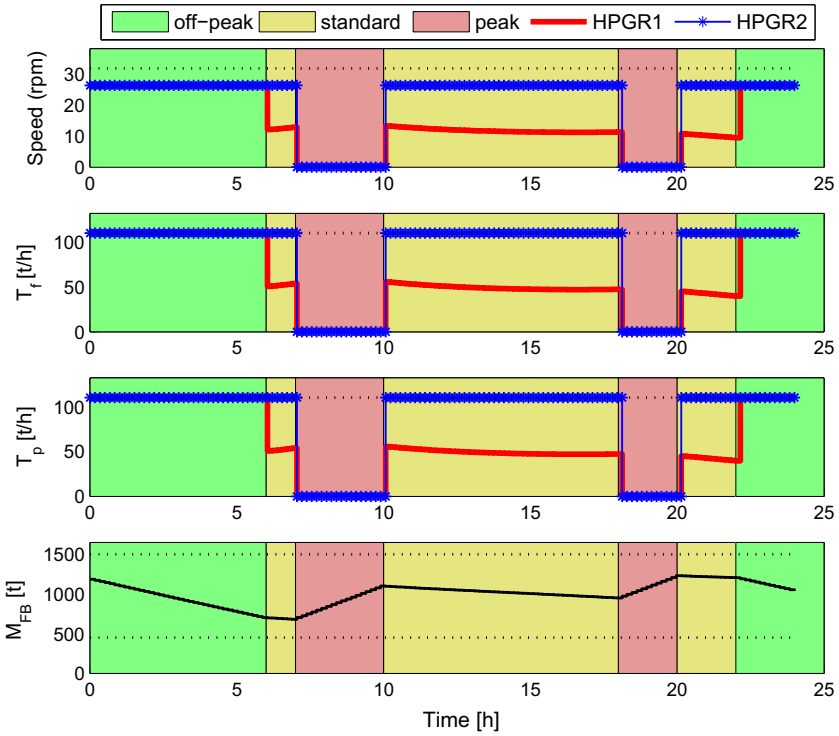

Fig. 9. Systems optimization control technique with different overall drive efficiency, $\eta_1 = 76\%, \eta_2 = 80.28\%$ using *linprog* function of Matlab Optimization Toolbox.

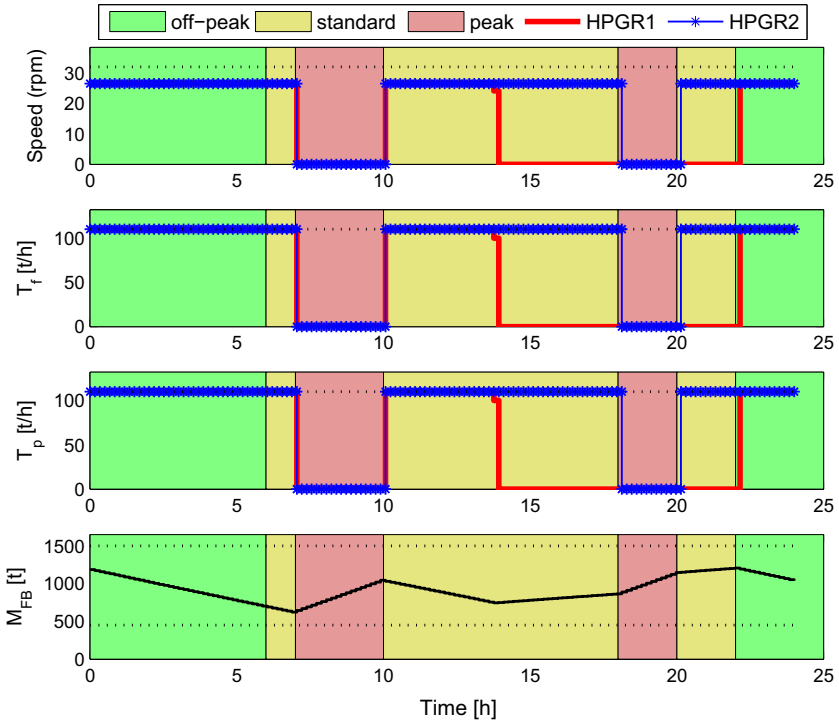

Fig. 10. Systems optimization control technique with different overall drive efficiency, $\eta_1 = 76\%, \eta_2 = 80.28\%$ using *opti* function of Opti Toolbox.

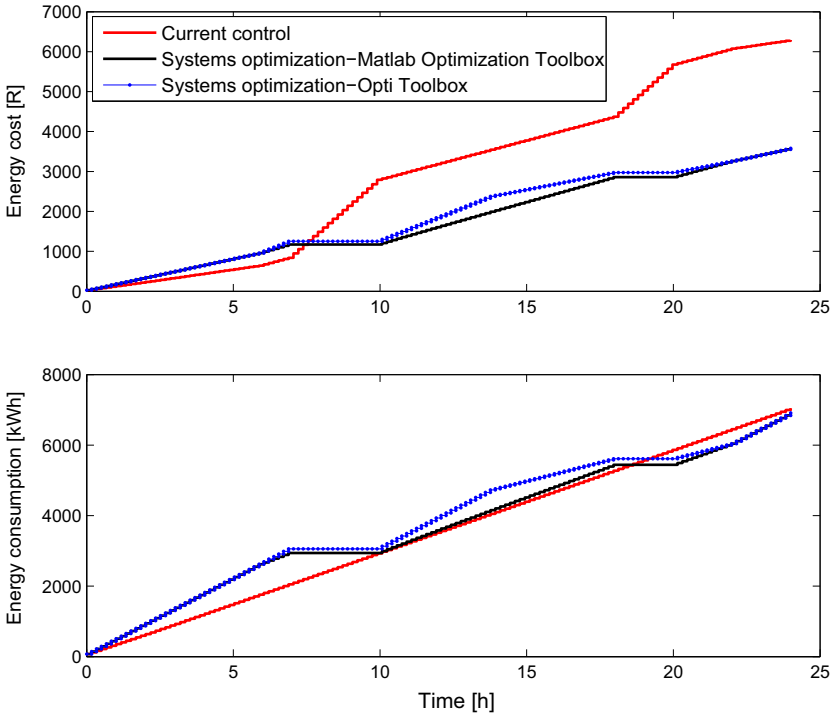

Fig. 11. Cumulative energy cost and consumption with different overall drive efficiency, $\eta_1 = 76\%, \eta_2 = 80.28\%$.

standard time for energy cost minimization. However, unlike Case I, the same figure shows that the optimization techniques detects the discrepancy between the two machine's overall efficiency and therefore runs HPGR2, which has higher overall efficiency at higher loading level while HPGR1 is operated at lower loading level for most of the time due its lower overall efficiency. The reason of this is to reduce the system energy consumption. From multi-objective optimization point of view, smaller overall efficiency means bigger weight and bigger overall efficiency means smaller weight. This is due to the fact that the overall efficiency is inversely proportional to the electric power consumption as shown in Eq. (9). Fig. 11 shows a reduction in both energy cost and energy consumption. As shown in Tables 8 and 9, the corresponding energy cost saving is 43.17% and energy saving is 1.87% for both

Table 7
Production and corresponding energy cost and consumption with different overall drive efficiency, $\eta_1 = 76\%, \eta_2 = 80.28\%$.

Technique	Production (t)	Energy cost (R)	Energy consumption (kW h)	Simulation time (s)
Current control	3500.2	6292.3	7045.7	/
Systems optimization using *linprog* function	3500.0	3579.2	6913.0	0.308
Systems optimization using *opti* function	3500.0	3579.2	6913.0	0.277

Table 8
Cost saving of systems optimization control technique with different overall drive efficiency, $\eta_1 = 76\%, \eta_2 = 80.28\%$.

Technique	Specific energy cost (R/t)	Cost saving (%)
Current control	1.7977	/
Systems optimization using *linprog* function	1.0226	43.17
Systems optimization using *opti* function	1.0226	43.17

Table 9
Energy saving of systems optimization technique with different overall, $\eta_1 = 76\%, \eta_2 = 80.28\%$.

Technique	Specific energy consumption (kW h/t)	Energy saving (%)
Current control	2.0129	/
Systems optimization using *linprog* function	1.9752	1.87
Systems optimization using *opti* function	1.9752	1.87

optimization techniques. The small increase in energy cost saving of about 1.24% compared to Case I (41.93%) comes from the 1.87% energy saving and the rest comes from load shifting.

Similarly to Case I, with *lingrop* function, the crusher with lower efficiency (HPGR1) is smoothly operated at a reduced loading level of about 50 t/h during standard periods while with *opti* function, the machine is switched on and off between its maximum and minimum loading levels.

In practice, however, the feasibility of the proposed model in saving the energy under this scenario depends on the predictability of the overall drive efficiency of each HPGR crusher with respect to the feed characteristics and feeding condition.

4.2.3Case III: Sensitivity of rolls operating pressure on energy and cost savings

As discussed in Section 2.3, the rolls operating pressure is the unique control variable affecting the specific energy consumption of the HPGR crusher. However, owing to the trade-off between the energy consumption and the product quality (product particle size distribution), any attempt in decreasing the HPGR energy consumption by decreasing the rolls operating pressure will lead to coarser particles in the product. In this scenario, small variations in rolls operating pressure on HPGR energy saving and product particle size distribution are investigated. The product particle size distribution is based on the modified Rosin-Ramler Bennets' distribution, expressed as a function of rolls operating pressure as given in Ref. [29]. The rolls operating pressure is decreased from 4.5 N/mm^2 to 3.5 N/mm^2 with a step of 0.2 N/mm^2. The overall efficiency of the two HPGR machines is the same as in Case I ($\eta_1 = \eta_2 = 80.28\%$). Simulation results are shown in Figs. 12–14. It can be seen from Fig. 12 that a small decrease in rolls operating pressure leads to considerable energy consumption and cost reduction without significant change in product particle size distribution as shown in Fig. 13. The actual savings obtained are shown in Fig. 14. This figure shows that for every 0.2 N/mm^2 decrement in rolls operating pressure, the energy saving and energy cost saving linearly increase by approximately 4.5% and 2.6%, respectively, while the product quality remain almost unaltered. For a total decrement in rolls operating pressure of 1 N/mm^2, an energy saving of 22.72% and energy cost saving of 55.13% are achieved.

However, in practice, in order to achieve the energy saving of HPGR process through small change in rolls operating pressure by maintaining the product quality performance, a high accurate regulatory controller is required to track and maintain the desired small changes in rolls operating pressure.

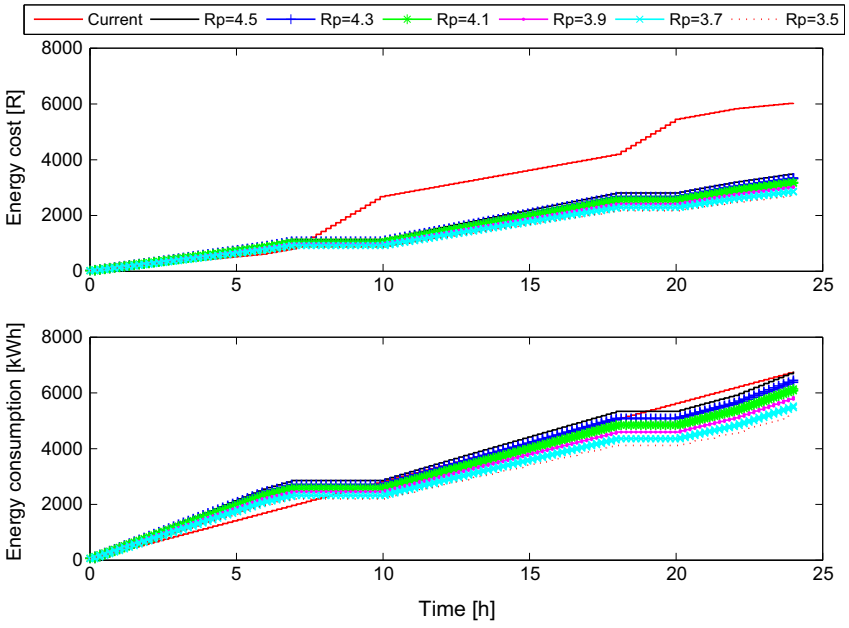

Fig. 12. Sensitivity of rolls operating pressure on cumulative energy cost and energy consumption.

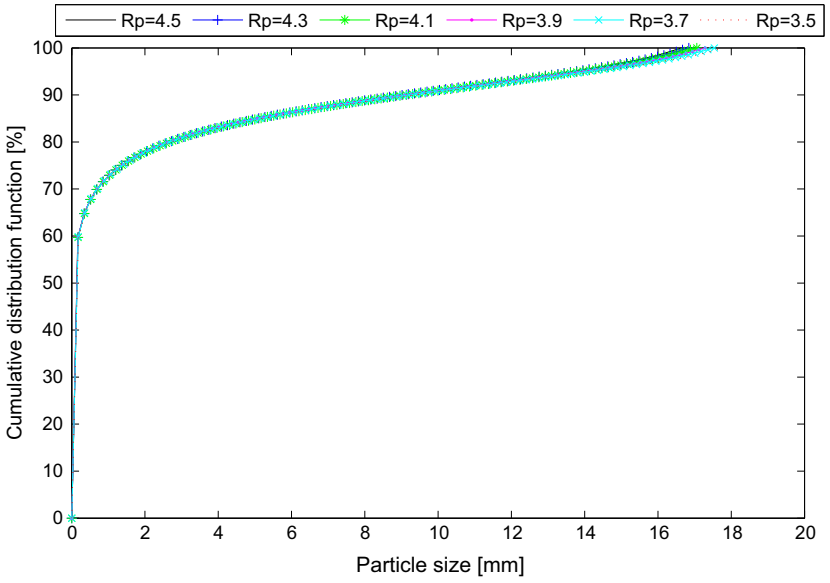

Fig. 13. Sensitivity of rolls operating pressure on product size distribution.

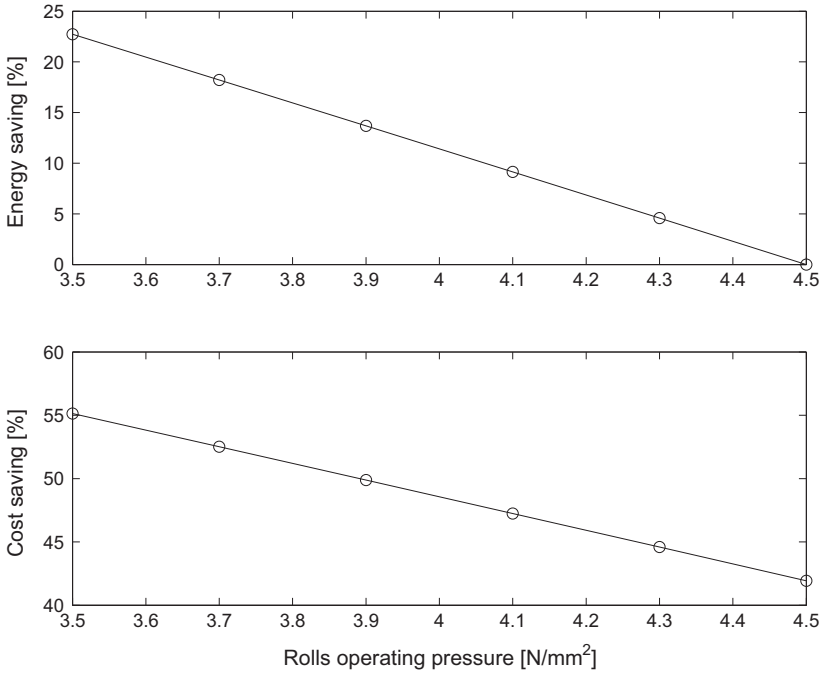

Fig. 14. Sensitivity of rolls operating pressure on energy and cost savings.

5. Conclusion

A systems optimization control model is proposed for energy management of a parallel HPGR crushing process. A case study of a tertiary copper crushing process is formulated and solved under three different scenarios.

In the first scenario where the two HPGRs are assumed to have equal overall drive efficiency with a fixed rolls operating pressure, simulation results reveal a potential of reducing the specific energy cost of about 41.93% without any energy consumption reduction.

In the second scenario where the overall drive efficiency of the two parallel HPGR are different with a fixed rolls operating pressure, it is shown that the energy saving is achieved by minimizing the loading level of the less-efficient HPGR machine and maximizing the loading level of the more-efficiency HPGR machine. A potential of energy saving of 1.87% and energy cost saving of 43.17% is shown.

In the last scenario where the sensitivity of rolls operating pressure is investigated on the trade-off between energy saving and product quality, it is shown that the specific energy consumption of HPGR is more sensitive to the change in rolls operating pressure than the product quality is. For any small decrement of 0.2 N/mm^2 in rolls operating pressure, a potential of 4.5% increase in energy saving is shown without significant change in product quality.

Acknowledgments

The authors would like to thank the National Research Foundation (NRF) of South Africa for financial support under grant unique number 88744. The support from the National Hub for Energy Efficiency and Demand Side Management (EEDSM) is also acknowledged.

References

[1] Borell M, Bäckström P-O, Söderberg L. Supervisory control of autogenous grinding circuits. Int J Miner Process 1996;44–45:337–48.
[2] Lestage R, Pomerleau A, Hodouin D. Constraint real-time optimization of a grinding circuit using steady-state linear programming supervisory control. Powder Technol 2002;124:254–63.
[3] Chen X-s, Li Q, Fei S-m. Supervisory expert control for ball mill grinding circuits. Expert Syst Appl 2008;34:1877–85.
[4] Radhakrishnan VR. Model based supervisory control of a ball mill grinding circuit. J Process Control 1999;9:195–211.
[5] Matthews B, Craig I. Demand side management of a run-of-mine ore milling circuit. Control Eng Pract 2013;21(6):759–68.
[6] Middelberg A, Zhang J, Xia X. An optimal control model for load shifting – with application in the energy management of a colliery. Appl Energy 2009;86:1266–73.
[7] Zhang S, Xia X. Optimal control of operation efficiency of belt conveyor systems. Appl Energy 2010;87(6):1929–37.
[8] Zhang S, Xia X. Modeling and energy efficiency optimization of belt conveyors. Appl Energy 2011;88(9):3061–71.
[9] Badenhorst W, Zhang J, Xia X. Optimal hoist scheduling of a deep level mine twin rock winder system for demand side management. Electr Power Syst Res 2011;81(5):1088–95.
[10] Numbi BP, Zhang J, Xia X. Optimal energy management for a jaw crushing process in deep mines. Energy 2014;68:337–48.
[11] Aske EMB, Strand S, Skogestad S. Coordinator MPC for maximization plant throughput. Comput Chem Eng 2008:32195–204.
[12] Serralunga FJ, Mussati MC, Aguirre PA. Model adaptation for real-time optimization in energy systems. Ind Eng Chem Res 2013;52:16795–810.
[13] van Staden AJ, Zhang J, Xia X. A model predictive control strategy for load shifting in a water pumping scheme with maximum demand charges. Appl Energy 2011;88(12):4785–94.
[14] Zhang H, Xia X, Zhang J. Optimal sizing and operation of pumping systems to achieve energy efficiency and load shifting. Electr Power Syst Res 2012;86:41–50.
[15] Zhuan X, Xia X. Optimal operation scheduling of a pumping station with multiple pumps. Appl Energy 2013;104:250–7.
[16] Zhuan X, Xia X. Development of efficient model predictive control strategy for cost-optimal operation of a water pumping station. IEEE Trans Control Syst Technol 2013;21(4):1449–54.
[17] Fuertstenau DW, Abouzeid A-ZM. Role of feed moisture in high-pressure roll mill comminution. Int J Miner Process 2007;82:203–10.
[18] Lindqvist M. Energy considerations in compressive and impact crushing of rock. Miner Eng 2008;21(9):631–41.
[19] Fuertstenau DW, Abouzeid A-ZM. The energy efficiency of ball milling comminution. Int J Miner Process 2002;67:161–85.
[20] Daniel MJ, Morrell S. HPGR model verification and scale-up. Miner Eng 2004;17:1149–61.
[21] Abouzeid A-ZM, Fuertstenau DW. Grinding of mineral mixtures in high-pressure grinding rolls. Int J Miner Process 2009;93:59–65.
[22] Hasanzadeh V, Farzanegan A. Robust HPGR model calibration using genetic algorithms. Miner Eng 2011;24:424–32.
[23] Dundar H, Benzer H, Aydogan N. Application of population balance model to HPGR crushing. Miner Eng 2013;50–51:114–20.
[24] Xia X, Zhang J, Cass W. Energy management of commercial buildings – a case study from a POET perspective of energy efficiency. J Energy Southern Afr 2012;23(1):23–31.
[25] Ashok G, Denis Y. Mineral processing design and operations: an introduction. Amsterdam, Boston: Elsevier; 2006.
[26] Londoño JG, Knights PF, Kizil MS. Modelling of in-pit crusher conveyor alternatives. Min Technol 2013;122(4):193–9.
[27] IEC. Rotating electrical machines-Part 30-1: efficiency classes of line operated AC motors (IE code). 1st ed. International Electrotechnical Commission; 2014.
[28] Torres M, Casali A. A novel approach for the modelling of high-pressure grinding rolls. Miner Eng 2009;22:1137–46.
[29] Saramak D. Mathematical models of particle size distribution in simulation analysis of high-pressure grinding roll operations. Physicochem Probl Miner Process 2013;49:121–31.
[30] Strejc V. Least squares parameter estimation. Automatica 1980;16:535–50.
[31] Saramak D, Kleiv RA. The effect of feed moisture on the comminution efficiency of HPGR cirsuits. Miner Eng 2013;43–44:105–11.
[32] Drozdiak JA. A pilot-scale examination of a novel high pressure grinding roll/stirred mill comminution circuit for hard-rock mining applications. M.A.Sc. thesis, Faculty of Graduate Studies (Mining Engineering), University of British Columbia, Vancouver, Canada; 2011.
[33] Van der Meer FP, Maphosa W. High pressure grinding moving ahead in copper, iron, and gold processing. J Southern Afr Inst Min Metall 2012;112:637–47.
[34] CEMA. Belt conveyors for bulk materials. 5th ed. United States: Conveyor Equipment Manufacturers Association; 2002.
[35] De Almeida AT, Ferreira FJTE, Both D. Technical and economical considerations in the application of variable-speed drives with electric motor systems. IEEE Trans Ind Appl 2005;41:188–99.
[36] Rule CM, Minnaar DM, Sauermann GM. HPGR-revolution in platinum. J Southern Afr Inst Min Metall 2009;108:23–30.